JCSE The Journal of Corrosion Science and Engineering
ISSN 1466-8858 Volume 19, Preprint 68 submitted7 October 2016

Redesign and Construction of Corrosion Cell for Improved Measurement of Corrosion Under Insulation

Gabriel ESSIEN[1], Richard BARKER[2] and Anne NEVILLE[3]

School of Mechanical Engineering, Oilfield Corrosion Engineering, University of Leeds, UK.
[Emails: gpessien@yahoo.com[1]; r.j.barker@leeds.ac.uk[2]; a.neville@leeds.ac.uk[3]]

ABSTRACT

Thermal insulation materials are used to insulate process equipment in petroleum and chemical industries usually with the objective to conserve heat for process control, reduce energy costs and protect personnel against noise, heat and cold burns. The ingress of water into insulation results in severe and hidden corrosion under insulation (CUI) material. This project is focused on construction of a modified CUI cell for laboratory investigation of corrosion under insulation. The implementation of the new cell recorded open circuit potential (OCP) and corrosion rate measurement for carbon steel insulated with mineral wool. The test sample showed low corrosion rates with predominance of corrosion spikes at high temperatures. Post-test inspection of corroded sample surface indicated the presence of uniform and localized corrosions especially at the top part of carbon steel sample.

Keywords: *Corrosion Under Insulation, CUI, Corrosion Cell, Design, Corrosion Measurement*

1.0 INTRODUCTION

The major material used for construction of facilities in the oil and gas industry is carbon steel because of its low cost, availability and desired mechanical properties [1]. The corrosion of oil facilities is inevitable because of the severe operating conditions and aggressive environment, which characterize the operations in the oil and gas industry [2]. These operating conditions are predefined to enable the processing, transportation or storage of hydrocarbons [3]. To maintain these

operating conditions, the process facilities especially piping are insulated to reduce the heat losses between these facilities and the surrounding. These insulated process facilities undergo corrosion when there is water ingress into the insulation material. Corrosion under insulation is a hidden and severe type of corrosion that accounts for more than 40% of pipeline maintenance cost in a typical process industry [4,5]. Corrosion under insulation (CUI) is the external

JCSE The Journal of Corrosion Science and Engineering
ISSN 1466-8858 Volume 19, Preprint 68 submitted7 October 2016

corrosion of piping and vessels made from carbon steels and austenitic stainless steels that occurs underneath the external insulation due to water penetration [6]. The corrosion rate for CUI has been reported to be 1.5 to 3.0 mm/year at 60-120 °C operating temperature [10]. The rate of corrosion is affected by oxygen, temperature, insulation contaminants (chlorides/sulphates), water permeability, wettability and retention [7]. The corrosion under insulation can occur at any temperature that allows moisture accumulation on surfaces of the insulated facilities. In spite of the advancement in research and development of CUI inspection and control methods, CUI still remains a challenging problem in the oil industry because of its unseen nature, delayed consequence and the culture of being ignored by inspection/management teams [8]. This project is focused on the design, construction and implementation of a corrosion cell for investigation of corrosion under insulation. The proposed design is based on the method provided by ASTMG 189 for investigation of CUI [9]. The corrosion measurement test was conducted for carbon steel coupon that is insulated with mineral wool. The test conditions were chosen to simulate a typical oilfield marine environment. The new cell will provide thermodynamic and kinetic data that will enable the study of mechanisms that drive the initiation of CUI. The understanding of these mechanisms and processes will enhance the prediction and protection oil facilities against CUI.

2.0 MATERIALS AND METHODS

Prior to redesign and construction of the CUI cell, a technical review of the ASTM 189 CUI test rig was carried out. This CUI test rig consist of two cells connected in series and a solution reservoir provided for wetting the insulation material. One of the two cells serves as the control for comparison while other is used for the actual test measurement as shown in Figure 1. The CUI cell was also provided with a heater, temperature controller and thermocouple to allow for temperature variation and measurement during testing.

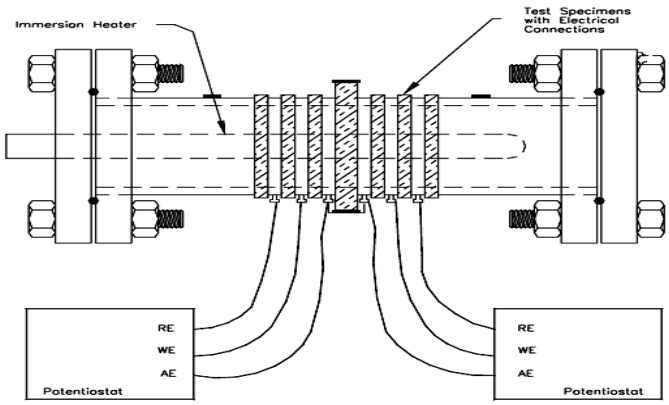

Figure 1: Schematic showing electrodes with electrical connections for CUI cell [11].

However, the simultaneous testing with the two cells may extend the error margin during measurement since both cells will be affected by error at the same time. Another important feature of the present CUI cell is the use of carbon steel sample material as

ISSN 1466-8858 Volume 19, Preprint 68 submitted7 October 2016

the reference and counter electrodes.

This is contrary to the non-oxidation criteria for selection of metals used for reference and counter electrodes. This arrangement is expected to vary the reference potential and subsequent polarization measurements.

2.1 Key Modifications and Improvements Added

The modified CUI cell will add the following improvements:

(i) From Figure 1, the carbon steel reference and counter electrodes were replaced by Silver/Silver Chloride (Ag/AgCl) standard reference electrode (Figure 2) for improved measurement of reference potential and corrosion rates.

(ii) The new constructed CUI cell is made of a single cell to ensure portability, simplicity, repeatability and flexibility of CUI measurements (Figure 2).

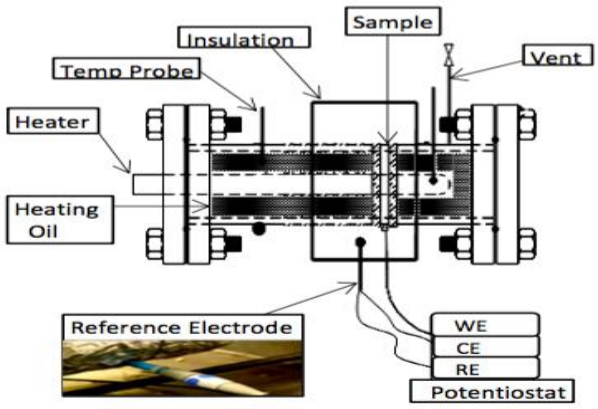

Figure 2: Schematic showing modified CUI cell

2.2 Construction of CUI Cell

The CUI cell was constructed from two inch (5.1cm) carbon steel pipe (En3B) with a test sample machined from the same pipe having a nominal length of 8.9 cm, wall thickness 0.5cm and exposed specimen surface area of 170cm^2 as shown in Figure 3.

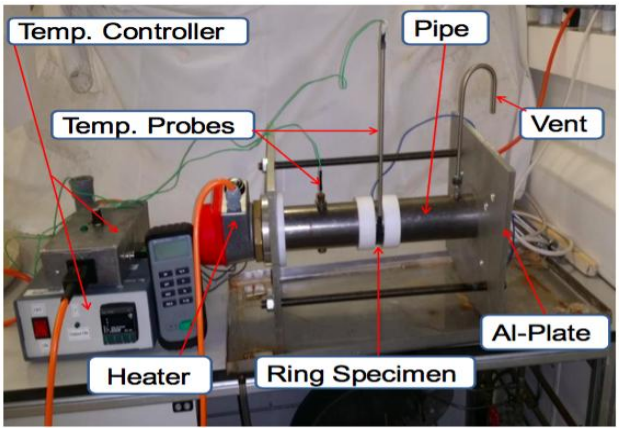

Figure 3: New Constructed CUI cell

The test sample was separated from the other pipe sections using spacers made of polytetrafluoroethylene resin. The test assembly was bolted and held together by studs passing through the aluminium plate attached to both ends of the flanged pipe.

The test temperature at the sample surface was achieved with the provision of temperature controller, thermocouples and immersion heater inserted into the pipe filled with special heating oil. The maximum allowable working temperature of the new CUI cell is 90^{o}C. The insulation material used was water-resistant mineral wool insulation. The design safety considerations for construction of the above CUI are documented in the risk assessment report contain in the main work.

JCSE The Journal of Corrosion Science and Engineering
ISSN 1466-8858 Volume 19, Preprint 68 submitted7 October 2016

2.3 Experimental Setup

The test apparatus was the constructed CUI Cell for measurement of corrosion under insulation on the outer surface of carbon steel sample as shown in Figure 4.

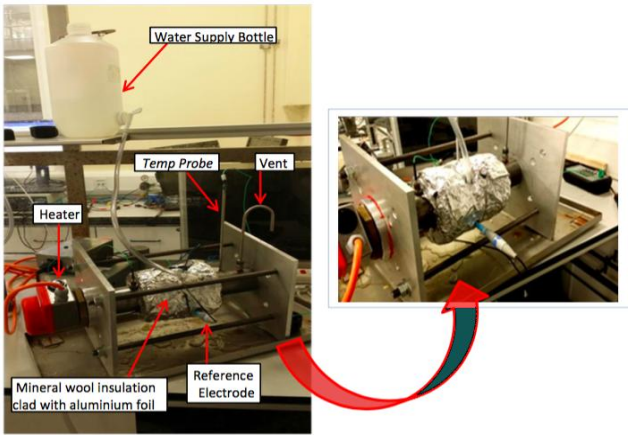

Figure 4: Experimental setup of constructed CUI cell

The CUI cell has a water supply bottle containing the aqueous test solution made of tap water with 3.5% NaCl and a pH of 4.5 adjusted using sulphuric acid. Water repellent mineral wool insulation was wrapped around the test sample with adequate sealing to retain supplied solution in order to wet and saturate the insulation material during testing. The electrodes of the CUI cell setup were connected to the potentiostat.

2.4 Test Procedures

The surface of the test sample was polished to 1200 grit finish with silicone paper and degreased with acetone, air dried and followed by measurement of initial sample mass. The test rig was assembled; pipe was filled with the heating oil and wrapped with mineral wool insulation saturated with water. The standard reference electrode was inserted at bottom of insulated pipe and sealed to retain test solution during measurement. Droplets of test solution were added to insulation to sustain continuous water saturation. The electrode terminals were wired to potentiostat and the CUI cell was aged for 72hrs prior to measurement. After the aging treatment, daily repeated measurement of open circuit potential (OCP) and corrosion rate was conducted for 5.6hrs each at cyclic temperature of 25±2°C and 60±2°C for 16 days exposure period. The repeated measurement on fixed sample is to mimic real life CUI situations in an oilfield. The exposed hot surfaces of test rig were covered with insulating blanket during testing to avoid possible burns to other lab users. At the end of testing, the mineral insulation was removed for post-test visual examination of corroded sample surface followed by removal of iron oxides with Clarke's solution and weighing of sample to obtain the final mass after measurement. All measured data before and after testing were recorded.

3.0 RESULTS AND DISCUSSION

The open circuit potential measurements and corrosion rate measurements for the test conditions are presented below.

3.1 Open Circuit Potential (OCP) Measurement.

The eight repeated OCP measurements

JCSE The Journal of Corrosion Science and Engineering
ISSN 1466-8858 Volume 19, Preprint 68 submitted7 October 2016

versus time at 25±2°C conducted on a daily basis for the test duration are shown in Figure 5.

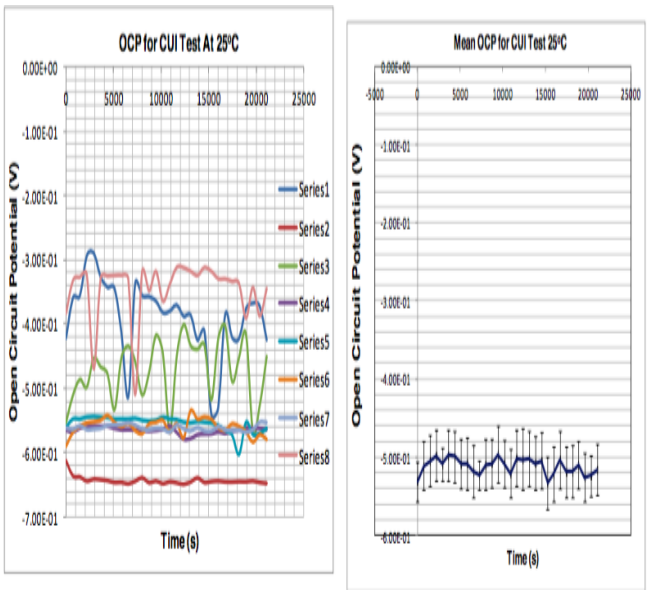

Figure 5: OCP Measurements at 25±2°C

Figure 5 shows the graphical plot of eight OCP readings versus time at 25°C which indicated deviation of some OCPs from the mean OCP of -0.511V. A more positive OCP of -0.313V (series-8) suggests possible ennoblement or passivation at the metal surface while a more negative OCP of -0.645V (series-2) indicates activeness and susceptibility to corrosion. This phenomenon confirms the likely semi-protective behaviour of the iron oxides formed on the sample surface. This finding is further supported by the unstable nature of some OCP readings (series1,3,8) which indicates possible breakdown or non-uniform formation of the oxide films. This action will promote corrosion in small local areas such as pitting and crevice corrosion.

3.2 The Open Circuit Potential (OCP) at 60±2°C

The eight repeated OCP measurements versus time at 60±2°C conducted on a daily basis for the test duration are shown in Figure 6.

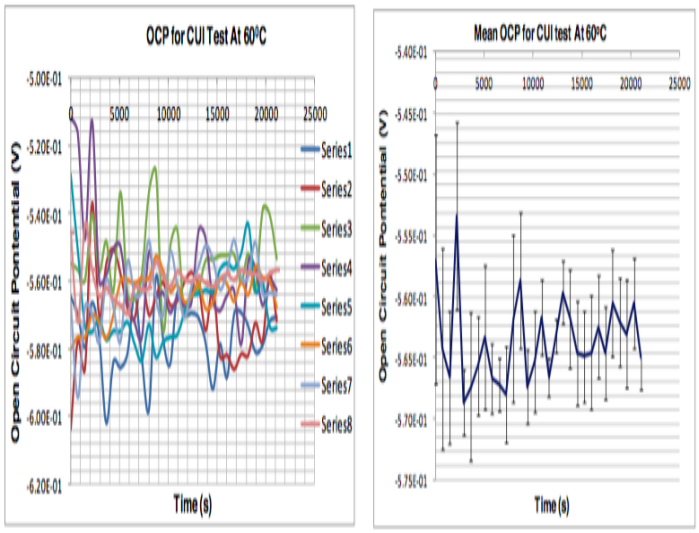

Figure 6: OCP Measurements at 60±2°C

Figure 6 shows the graphical plot of eight OCP readings versus time at 60°C. This plot indicates fewer deviations from the mean OCP of -0.564V compared to OCP readings at 25°C. However, the graph shows significant instability of the OCP measurements compared to OCP measurements at 25°C. This is may be due to the variability of the corrosion activity at the metal surface caused by multiple breakdowns of oxide films and the corrosion of these local areas on metal surface. This increased susceptibility to corrosion activities is confirmed by the higher mean OCP at 60°C compared to

ISSN 1466-8858 Volume 19, Preprint 68 submitted7 October 2016

mean OCP at 25°C. Based on these observations, one can infer that insulated steels subjected to high cyclic temperature services are more prone to CUI attack/failures. Besides, this finding agrees with published data on increase of corrosion rate with temperature [14].

3.3 Corrosion Rate Measurement at 25±2°C

The eight readings of corrosion rates versus time at 25±2°C measured on a daily basis for carbon steel sample under wetted insulation material is shown in Figure 7.

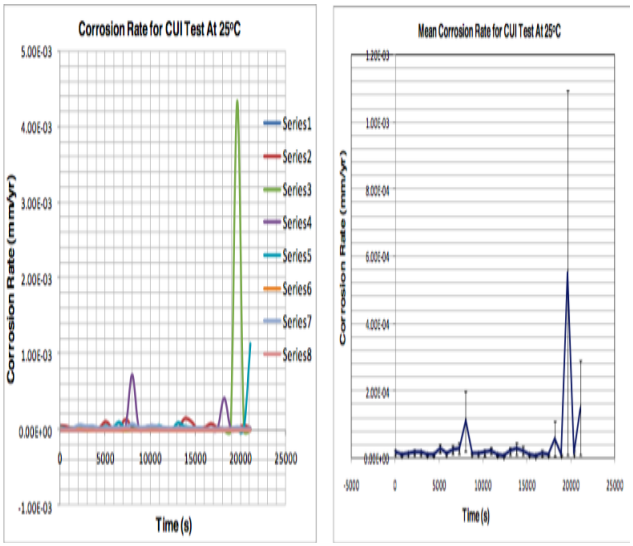

Figure 7: Corrosion rate measurement at 25±2°C

Figure 7 shows the graphical plot of eight corrosion rate measurements versus time at 25°C. This plot indicates infinitesimal corrosion rates having a mean value of 4.15E-05mm/yr. The low corrosion rates as seen on graph were stable with few corrosion spikes, which suggest the uniformity and stability of the corrosion process on sample at 25°C. Hara et al [12] and Kehler et al [13] confirmed the presence of corrosion spikes to indicate initiation of localized corrosions.

The formation of these localized cells may be due to changes in concentration, temperature or breakdown of protective films at local areas. The low corrosion rates recorded may be due to formation of protective films which is confirmed in this study by the significant oxide layers observed on sample surface after testing. However, one would expect to see an initial increase in corrosion rate followed by subsequent reduction due to formation of protective films. This initial corrosion may have occurred during the three days ageing of test sample prior to CUI measurement including other idle times of the test rig thereafter. Another likely contributor to this low corrosion rates is the high polarization resistance (R_P), which may be due to dissolved minute particles of insulation material in the electrolyte. However, no experiment was conducted to confirm this activity.

3.4 Corrosion Rate Measurement at 60±2°C

The eight readings of corrosion rates versus time at 60±2°C measured on a daily basis for carbon steel sample under wetted insulation material is shown in Figure 8.

ISSN 1466-8858 Volume 19, Preprint 68 submitted7 October 2016

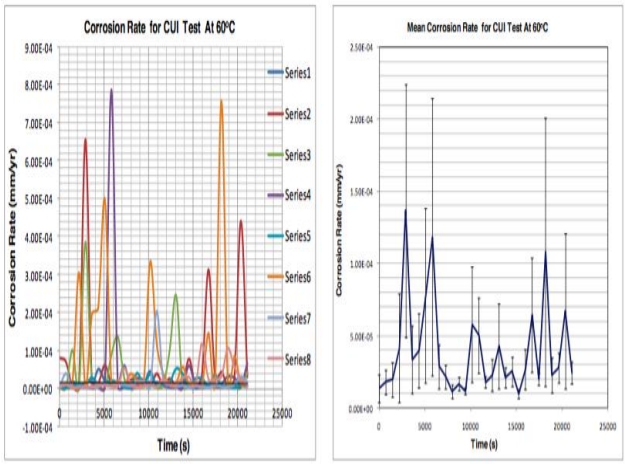

Figure 8: Corrosion rate measurement at 60±2°C

This plot also shows low corrosion rates with a mean value of 3.98E-05mm/yr. This value was slightly lower than the mean corrosion rate recorded at 25°C. The slight reduction in corrosion rate may be due to evaporation of test solution and the decrease of oxygen concentration with temperature at the metal surface. Furthermore, the measured corrosion rate at 60°C showed predominance of spikes. As mentioned earlier, the presence of corrosion spikes suggests likely initiation of localized corrosions such as pitting, crevice or galvanic corrosion. Besides, the numerous corrosion spikes confirm significant loss of protection offered by the protective films involving repeated breakdown and repair events. The recorded low CUI corrosion rate suggests the linear polarisation resistance measurement may not account for these localized corrosions as indicated by corrosion spikes. The substantial presence of corrosion spikes at high temperature agrees with the measured OCP at 60°C and also confirms localized corrosion as the controlling corrosion mode for CUI. The sustained life of localized corrosions at higher temperature compared to the room temperature is indicated by the large interval times between corrosion spikes (Figure 8 above). Each spike represents a localized cell and a group of spikes is expected to generate significant metal loss. These localized cells may be caused by changes in solution concentration and temperature at the metal-solution interface. The other contributing factors to formation of these localized cells may be changes in metal microstructure, presence of inclusions and damaged/uneven formation of the protective oxide layers.

3.5 Mass Loss Corrosion Rate Measurement.

The initial recorded mass of test sample was 801.5g and the final mass after testing and cleaning sample with Clarke's solution was 800.3g which netted to 1.2g mass loss for the tested sample. The following formula in Equation 1 is used to calculate corrosion rate from mass loss [15]:

$$CR\ (mm/yr) = 87.6 \times W/D \times AT \qquad 1.0$$

Where W is weight loss (mg), D is sample density (g/cm^3), A is sample surface area (cm^2) and T is the exposure time (hr). The calculated CUI corrosion rate based on mass loss for 16 days exposure period with sample surface area of 170cm^2 was 2.05E-

ISSN 1466-8858 Volume 19, Preprint 68 submitted7 October 2016

01mm/yr. This corrosion rate is higher than the ones obtained from linear polarisation resistance measurements. It is a good representative of the baseline or minimum general corrosion rate for the carbon steel sample insulated with mineral wool because it accounts for the overall mass losses due to uniform and some localized corrosions. However, this corrosion rate does not represent the rate of localized corrosions because badly pitted surface can exhibit negligible weight loss if attack is extremely localized. In practical terms, an increase in this calculated corrosion rate is anticipated.

3.6 Post Test Visual Evaluation

Sequel to the completion of CUI measurements, the surface of the test sample was examined to ascertain the extent of uniform or localized corrosions. The mineral wool insulation was removed from the CUI cell and the level of corrosion on test sample is as shown in Figure 9.

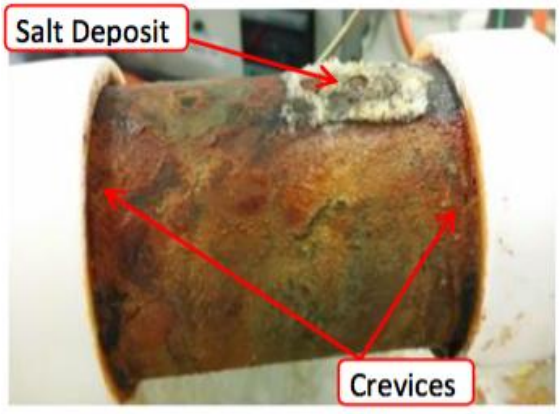

Figure 9: Schematic showing CUI on sample after testing

Figure 9 shows the presence of uniform and localized corrosions at the top positions of the test sample. Thick and dark rust stains were observed at crevices created at the sides of sample by insulation and joints between the Teflon spacer and test sample. Salt deposits were observed at the top part where solution was introduced to wet the insulation. These salt deposits are formed by concentration cells due to solution evaporation or drying at the top portion of the test sample. The considerable formation of iron oxides confirms the reduction in corrosion rates due to these oxide layers. However, experiment to determine the constituent of these protective oxides was not conducted. The evidence of localized corrosions such as pitting was observed on the test sample after cleaning the corroded surface with Clarke's solution (Figure 10).

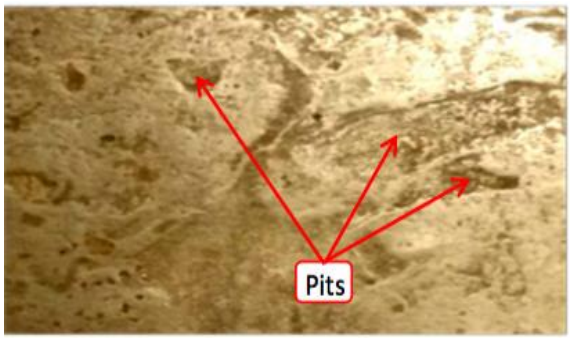

Figure 10: Schematic showing shallow pits on corroded sample after testing.

The other observations include the sticking of mineral wool insulation to test sample and also the presence of non-corroded areas on the sample surface (Figure 11).

ISSN 1466-8858 Volume 19, Preprint 68 submitted7 October 2016

Figure 11: Schematic showing stuck insulation on test sample with non-corroded areas.

The non-corroded areas of sample surface further confirm the presence of localized cells in CUI. Another likely promoter of these localized cells aside the ones mentioned in Section 3.3-3.4 is the hydrophobic property of mineral wool insulation. The hydrophobic chemical additives are added by manufacturers to repel water absorption in insulation. However, eventually when there is water ingress, this property tends to break and separate water into large droplets that will enhance formation of localized cells as can be seen in Figure 11 above. No experiment was conducted to confirm this activity.

4.0 CONCLUSION

Corrosion under insulation is a hidden and localized form corrosion that is difficult to predict and control which calls for new and/or improved methods of measurement, inspection, prevention and control. In this regard, a modified CUI cell was constructed and implemented for measurement of CUI. The constructed CUI cell recorded low corrosion rate for carbon steel insulated with mineral wool, lower OCP at high temperature and a higher corrosion rate from mass loss. This high corrosion rate from mass loss compared to corrosion rate from polarization measurements makes it a good representative of the actual CUI. Furthermore, the CUI cell implementation highlighted certain activities that will aid the understanding of CUI mechanism. This included the predominance of corrosion spikes at high temperature suggesting susceptibility to localized corrosions, variation in OCP indicating semi-protective behaviour of the oxide films, salt deposits alongside uniform and pitting corrosion seen on the top part of sample surface. The future application of the new cell using zero resistance technique or electrochemical noise technique will enable measurement of localized corrosion rate in CUI. The other future works for CUI control using the new cell will include modelling of CUI, selection of insulation materials, development and testing of protective coatings and embedded corrosion inhibitors. The accomplishment of aforementioned future works will result in sound prevention and control measures for CUI as a recipe to reduce failures and sustain productivity in the oil/gas industry.

ISSN 1466-8858 Volume 19, Preprint 68 submitted7 October 2016

5.0 ACKNOWLEDGEMENT

The contribution and support of Wood Group Integrity Management (WGIM) Company towards the success of this article is gratefully appreciated and acknowledged.

6.0 REFERENCES

1. Popoola, L.T., et al., *Corrosion problems during oil and gas production and its mitigation.* International Journal of Industrial Chemistry, 2013. 4(1): p. 35.
2. Garverick, L., *Corrosion in the petrochemical industry*. 1994: ASM international.
3. Speight, J.G. and B. Ozum, *Petroleum refining processes*. 2001: CRC Press.
4. Ahluwalia, H.S., *CUI: An In-Depth Analysis.* ASM Handbook, 2006. 13.
5. Fruge, D., et al. *Corrosion Under Insulation*. in *The 2008 Spring National Meeting*. 2008.
6. Winnik, S., *Corrosion under insulation (CUI) guidelines*. 2014: Elsevier.
7. Hanratty, T., *Corrosion under insulation is a hidden problem.* Hydrocarbon Processing, 2013. 92(3): p. 51-2.
8. Anderson, S.A., *Out of Sight, Out of Mind? Hydrocarbon Engineering.*, 2010.
9. *G189, "Standard Guide for Laboratory Simulation of Corrosion Under Insulation", ASTM International, West Conshohocken, PA.*, 2007.
10. Geary, W., *Analysis of corrosion under insulation failure in a carbon steel refinery hydrocarbon line.* Case Studies in Engineering Failure Analysis, 2013. 1(4): p. 249-256.
11. Kane, R.D., M. Chauviere, and K. Chustz, *Evaluation of Steel and Tsa Coating in A Corrosion Under Insulation (Cui) Environment*, NACE International.
12. Hara, N., et al., *Improvement of Pitting Corrosion Resistance of Type 316L Stainless Steel by Potentiostatic Removal of Surface MnS Inclusions.* International Journal of Corrosion, 2012. 2012.
13. Kehler, B., G. Ilevbare, and J. Scully, *Crevice corrosion stabilization and passivation behaviour of Alloy 625 and Alloy 22.* Corrosion, 2001. 57(12): p. 1042-1065.
14. Gerasimov, V. V., & Rozenfeld, I. L. (1957). *Effect of temperature on the rate of corrosion of metals. Russian Chemical Bulletin, 6(10), 1192-1197.*
15. *Fontana, M.G., Corrosion engineering. 2005: Tata McGraw-Hill Education*.